

Article

Energy and Exergy Analyses of a Combined Infrared Radiation-Counterflow Circulation (IRCC) Corn Dryer

Chengjie Li, Bin Li, Junying Huang and Changyou Li *

College of Engineering, South China Agricultural University, Guangzhou 510642, China; lichengjie@stu.scau.edu.cn (C.L.); libin@stu.scau.edu.cn (B.L.); huangjunying@stu.scau.edu.cn (J.H.)

* Correspondence: lichyx@scau.edu.cn; Tel.: +86-20-85280817

Received: 13 August 2020; Accepted: 7 September 2020; Published: 10 September 2020



Abstract: Energy consumption performance evaluation of an industrial grain dryer is an essential step to check its current status and to put forward suggestions for more effective operation. The present work proposed a combined IRCC dryer with drying capacity of 4.2 t/h that uses a novel drying technology. Moreover, the existing energy–exergy methodology was applied to evaluate the performance of the dryer on the basis of energy efficiency, heat loss characteristics, energy recovery, exergy flow and exergetic efficiency. The results demonstrated that the average drying rate of the present drying system was $1.1 \text{ g}_{\text{water}}/\text{g}_{\text{wet matter}} \text{ h}$. The energy efficiency of the whole drying system varied from 2.16% to 35.21% during the drying process. The overall recovered radiant energy and the average radiant exergy rate were 674,339.3 kJ and 3.54 kW, respectively. However, the average heat-loss rate of 3145.26 MJ/h indicated that measures should be put in place to improve its performance. Concerning the exergy aspect, the average exergy rate for dehydration was 462 kW and the exergy efficiency of the whole drying system ranged from 5.16% to 38.21%. Additionally, the exergy analysis of the components indicated that the combustion chamber should be primarily optimized among the whole drying system. The main conclusions of the present work may provide theoretical basis for the optimum design of the industrial drying process from the viewpoint of energetics.

Keywords: industrial grain dryer; exergy; energy; corn; dehydration

1. Introduction

Drying is a complicated thermodynamic process containing heat and mass transfer between the external constraints and inherent properties, which leads to the decrease of the moisture content of agricultural products or industrial material to a safe storage grade or to a grade appropriate for commercial use [1–3]. Due to the negative conditions such as the high latent heat of water evaporation and the relatively low efficiency of dryers, drying is a highly energy intensive operation that is an unneglected factor raising environmental concerns [4]. According to Tohidi [5], drying operations consumed about 10–15% of the total national industrial energy consumed in Canada, France and the USA, and 20–25% in Germany and Denmark. Therefore, like other energy-intensive industries, it is of great significance to search for energy-saving strategies and technologies to achieve the most effective and economic modes for drying industry.

Corn drying is a high-energy-consumption process that is very susceptible to the quality of processed corn. In recent years, investigators have conducted many studies of new drying equipment and techniques for the purpose of decreasing the energy consumption of the process and improving quality of product [6–10]. For example, Xie et al. [11] conducted in-depth explorations into the application of radio frequency-hot air drying technology on corn kernels in 2020 and found that a

reduced electrode gap can not only improve seed vigor, but also reduce specific energy consumption. Faria et al. [12] used microwave radiation to assess effects on the physiological quality of the seeds submitted to different drying conditions and indicated that drying with microwaves not only reduced the drying time of corn kernels, but also increased the longevity and the water absorption capacity of the seeds. Li et al. [13] developed an advanced hot air-drying method for corn kernels by using a pretreatment of low-temperature plasma and results showed that the low-temperature plasma pretreatment had a significant effect on drying kinetics. Although the new methods based on laboratory experiments have been reported as efficient drying methods for quality corn, the study results are still not suitable in industrial drying scale featuring a complex system composed of several parts. Moreover, since energy is an inaccessible factor in the realization of human sustainable development, it is of great significant to reveal the components and quantities of energy loss and exergy destruction in industrial drying system [14].

Traditionally, energy–exergy methodology is a useful tool which reveals where and to what extent more efficient drying systems can be designed by reducing the existing inefficiencies sources [15]. Energy analysis, which applies the first law of thermodynamics, has been commonly adopted in engineering systems performance analysis from the principle of conservation of energy. However, it gives no information about how to distinguish the quality of the energy [1,16]. Exergy refers to the maximum work that can be obtained when the material flow, heat flow or work reaches to equilibrium with the reference environment through a reversible process [17]. Since this is a method to analyze, design and improve energy and other systems by using the principles of conservation of mass and energy and the second law of thermodynamics, it is a more powerful tool for evaluating the effective use of energy. Compared with other energy analysis, the view of this process is more realistic [18]. Hence, based on the second law of thermodynamics and related theories, a large amount of research has been committed to evaluations of energy and exergy in the drying process [19–23]. For instance, Delgado-Plaza et al. [24] developed a hybrid dryer that utilizes a combination of different energy sources to optimize the drying process, while ensuring high-quality dried products. The result indicated that the efficiency of the equipment was around 60%. Darvishi et al. [25] studied the influence of relevant factors on the drying energy and exergy in the process of kiwifruit slices microwave drying and found that with the increase of microwave power and the decrease of slice thickness, the energy and exergy efficiency also increased. As far as we know, there is seldom articles published on energy and exergy analysis for corn drying, especially in case of industrial drying system.

Based on the above considerations, the present work proposed a combined IRCC corn dryer which adopts a novel drying technology. The existing energy–exergy methodology was applied to assess the energetic and exergetic performance of the drying system based on the first and second law of thermodynamics. The novel aspect of this study is, hence, providing the theoretical basis and the technical support for optimum design of the industrial drying process from the view point of energetics. The main conclusions may lay a foundation for developing the optimum controller of industrial grain drying system to obtain higher quality corn at acceptable energy consumption.

2. Materials and Methods

2.1. Materials

The fresh corn used in this project was a native variety named Changcheng 799#, as depicted in Figure 1, which was obtained from Zhencheng Farm at Xinzhou Shanxi Province, China. The impurities and broken seeds in the sample will be removed by the filter of the dryer before entering the dryer. The average initial moisture content (MC) was 27.95% w.b. measured by standard oven method [26].



Figure 1. Fresh corn sample for the experiment.

2.2. Principle and Process of Equipment

Given that corn is a heat-sensitive material, a reasonable drying mode for corn should be able to dry quickly and timely under conditions close to the environment temperature [27]. From the point of view of energy consumption of the structure of the corn drying process [10], the heat energy consumed by the water evaporation process of corn in the drying system must be accompanied by a reduction of its internal energy. The binding energy model constructed by Li [28] et al. indicates that in grains with low moisture content, the binding energy between the grain and its moisture is significantly affected by the drying temperature, while the water evaporation of grains with high moisture content is hardly limited by the grain itself.

Infrared radiation (IR) drying is an advisable method due to the fact that corn temperature is not restricted by the wet-bulb temperature of the medium [29]. Moreover, infrared heating has many potential merits over traditional drying, such as fast drying rate, acceptable energy efficiency, uniform product temperature and less dust-generation during drying process [30]. High grain temperatures can be obtained in a short time for quick dehydration, which results in the availability of high-quality grain.

Based on the above, the present work proposes a combined IRCC corn dryer that adopts a novel drying technology. Figure 2 describes the scene graph of IRCC corn dryer. The system consists of three main parts: heating section, drying chamber and dedusting section. The heating section mainly consists of an economical, durable and efficient combustion chamber using coal as fuel. More details about the self-developed combustion chamber can be found in the patent (CN105757650B) [31]. The tube row of the heat exchanger is a cross-row type, and its main part is a heat exchange pipe, with 11 columns \times 23 rows and a total of 253. There are two upper and lower diversion layers connected to the heat exchanger pipes. The size of the diversion layer is 2800 \times 1800 \times 450 mm. There are two baffles inside to divide it into three small chambers to conduct heat flow, respectively. This arrangement can ensure that the fluid flows through the tube bundle and increase the disturbance to improve the heat-transfer coefficient. In drying chamber, corn flows through the tempering section (TP), infrared radiation drying section (IRD), counterflow drying chamber (DC) and the discharging section (DCS) from top to bottom and then returns to the TP under the promotion of the hoist, which forms a grain circulation circuit. The IRD is mainly composed of four tubular infrared radiators (RA) which are inserted in the dryer and surrounded by flowing corn. The grain discharging section is composed of a reciprocating grain discharging device [32], which ensuring the self-cleaning of grain and the reduction of damage in the process of discharging. The medium after being heated by heat exchanger (HE) flows into the drying chamber and contacts with the corn to absorb moisture, which forms a medium flow circuit. The partial flue gas discharged from combustion chamber (CC) passes through the IRD, and the waste heat is used to heat corn. The exhaust gas discharged from DC and the exhaust flue gas discharged from IRD flow into the dust removal chamber under the promotion of the induced fan (Model 4-68,

Tongda, Inc., Linyi, China). The period of a circulation is about 90 min with drying capacity of about 4.2 t/h. The developed IRCC corn dryer has been put into application in Zhencheng Farm at Xinzhou Shanxi Province, China.

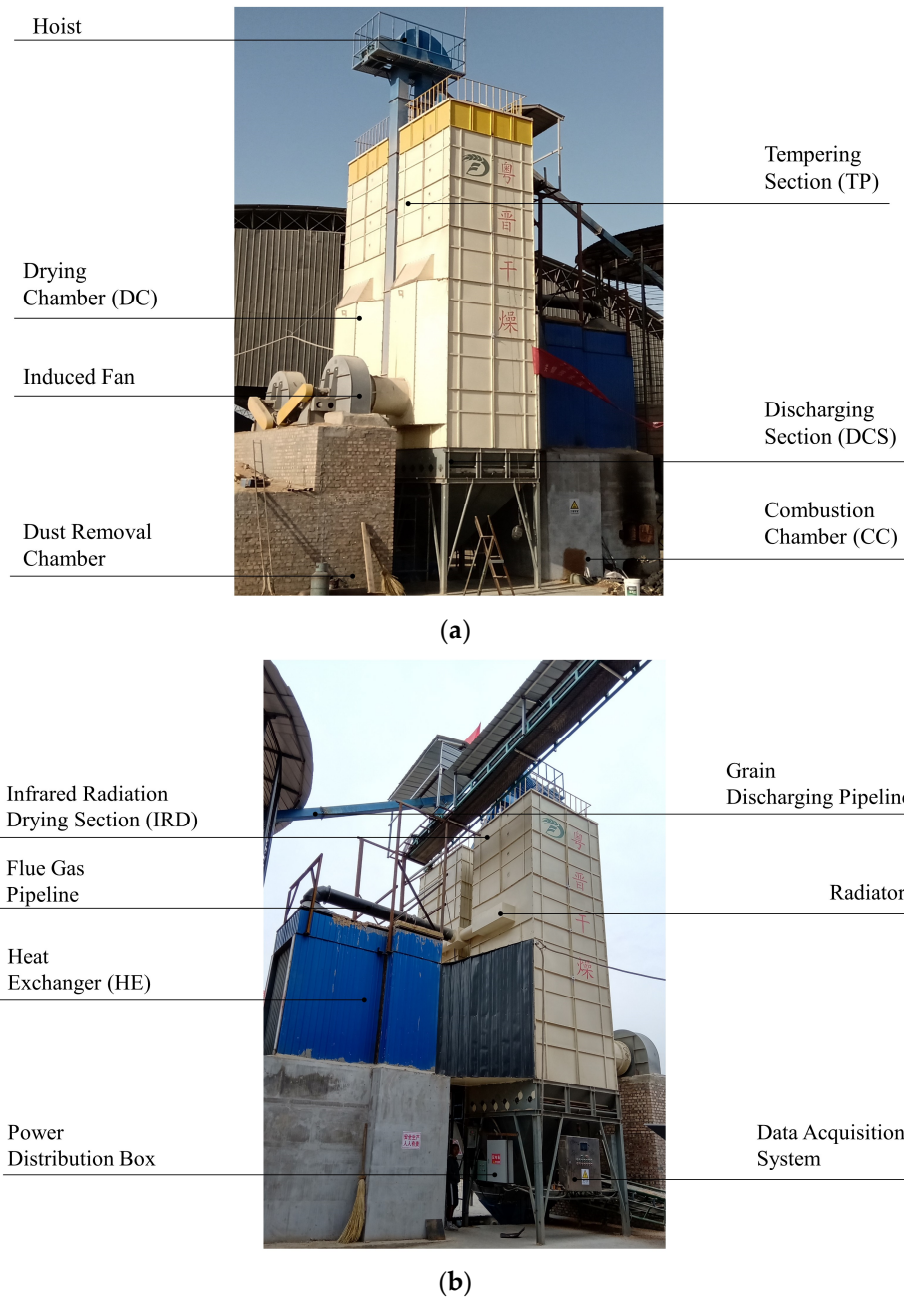


Figure 2. Diagram of the IRCC corn dryer. (a) Front; (b) rear.

2.3. Drying Procedure and Data Collection

A schematic diagram of the dryer is shown in Figure 3. As shown in the diagram, before drying, the corn to be dried is lifted to the inlet of the dryer under the action of the hoist and drops into the dryer cavity. After the dryer cavity is filled with corn, the drying officially begins as the induced fan, hoist and discharging motor are turned on in sequence. The corn is constantly dehydrated in the process of circulation flow. The temperature data used in the experiment including inlet air (T_{ai}), outlet air (T_{ao}), outlet corn (T_g), ambient (T_∞), radiator (T_r) temperature and humidity data including

inlet air (H_{ai}), outlet air (H_{ao}), ambient (H_{∞}) humidity were measured by the appropriate sensors, which were linked with the self-developed data acquisition system, as shown in Figure 3. The MC of the outlet corn were measured using the standard oven method [26]. According to the national standard GB 1353-2018 [33], the safe storage moisture content of corn is about 14% w.b. Therefore, when the detected moisture content of the outlet grain is about 14% w.b., the drying stopped and the product began to be discharged through the grain discharging pipeline, as shown in Figure 2b. All the experiment data were measured with a collection period of 30 min. The descriptions of the related experimental instruments are listed in Table 1.

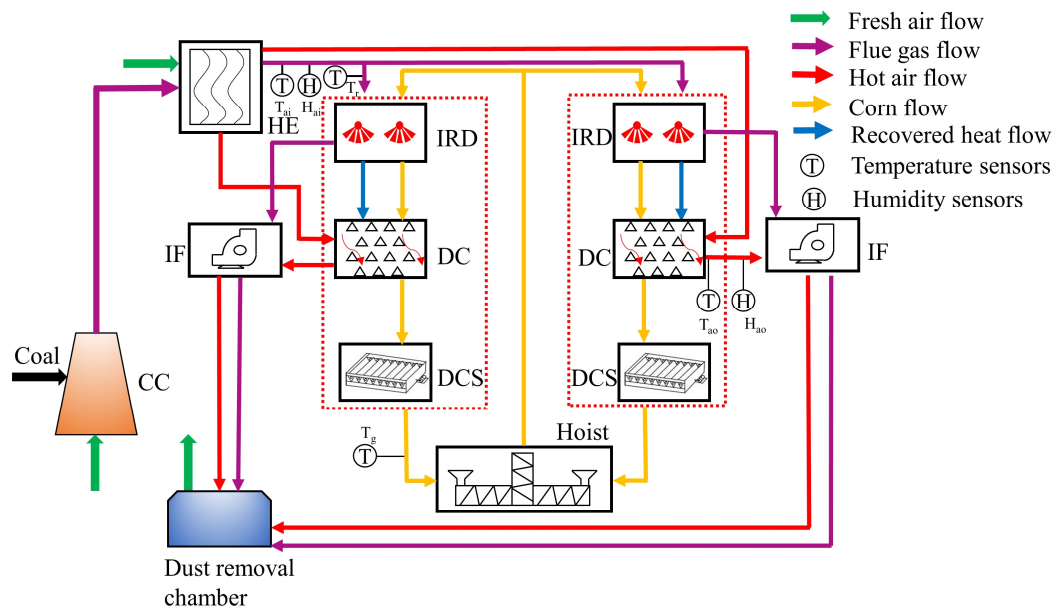


Figure 3. Thorough schematic view of the dryer and instrumentations assisted by energy and mass flow.

Table 1. Descriptions of the related experimental instruments.

Instruments	Model	Measurement Scope	Accuracy
Temperature resistance	PT100	−200–450 °C	±0.1 °C
Pyrometer couple	WRN-130/230	0–1300 °C	±0.1 °C
Anemograph	DT-8893	0.001–45 m/s	0.01 m/s
Temperature and humidity sensor	AM2301	0–100%/−40–80 °C	±3%/±0.5 °C
Data-acquisition system	Self-developed	–	–

2.4. Theoretical Principle Used for Energy and Exergy Analyses

The below hypotheses were completed for developing the solution scheme for the energy and exergy analyses equations of the corn drying system:

- The initial total weight of the corn in the dryer was regarded as 50 t;
- All components of the dryer were assumed to be operating in a stable state;
- The moisture of corn diffuses to the drying medium in the form of gas;
- The temperature potential inside a single corn kernel was ignored;
- The loss of heat stemming from inertia, convection and radiation in the drying chamber was ignored;
- The moisture (M_{ar}), oxygen (O_{ar}), ash (A_{ar}) content and low heat value (LHV) of coal used in the present project were assumed to be 8.0%, 3.19%, 19.02% and 28.073 MJ/kg, respectively [34].

2.4.1. Energy Analysis

The energy balance equation on account of the first law of thermodynamics was express as Equation (1) [35]:

$$\sum \dot{E}_{in} = \sum \dot{E}_{out} \tag{1}$$

The energy flow in the present hot air-drying system for corn is shown in Figure 4. According to the Equation (1) and Figure 4, the following equation was obtained:

$$\dot{Q} + \dot{P} = \dot{W} + E_{nevp} + \sum \dot{E}_{loss} \tag{2}$$

where \dot{Q} is the energy provided by the fuel, \dot{P} is the electrical energy provided by the power source, and \dot{W} is the work done by the hoist.

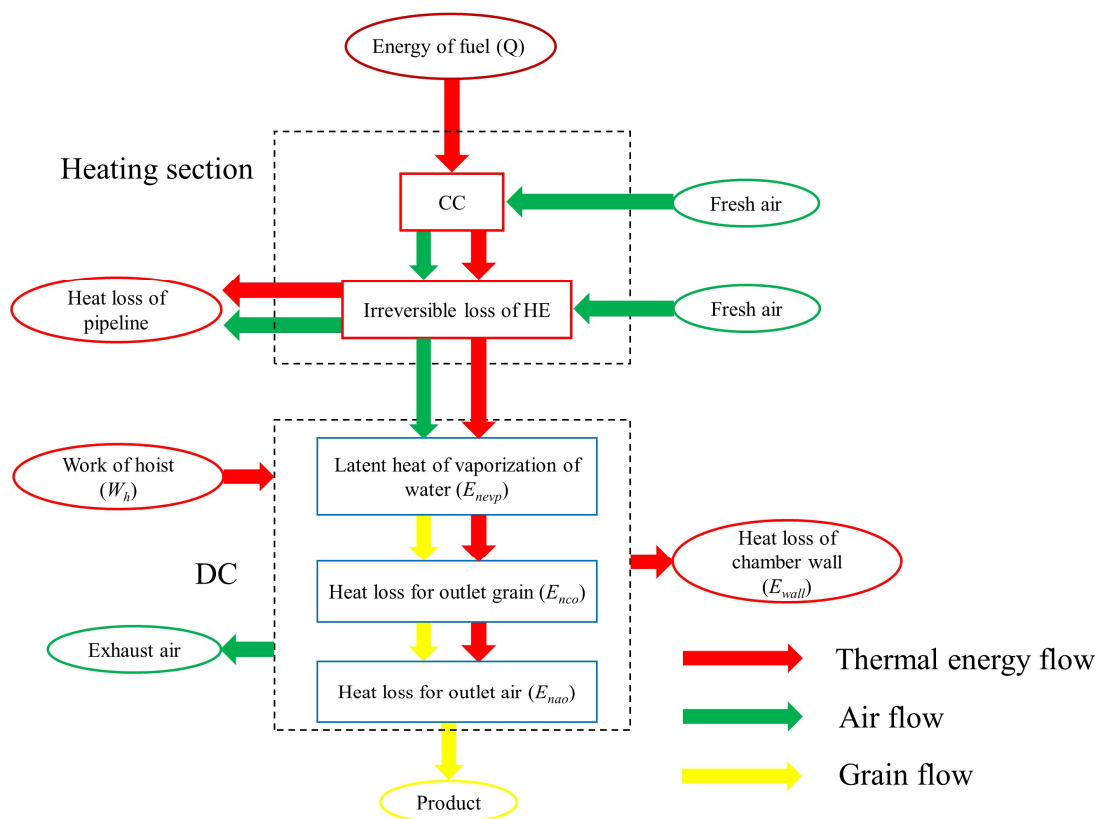


Figure 4. Energy flow in hot air-drying system for corn.

For the whole drying system, the total energy consuming element consists of \dot{Q} , the hoist (\dot{P}_h), the discharging motor (\dot{P}_{dm}), the induced fan (\dot{P}_{if}) and the additional parts (\dot{P}_{ap}), as shown in Figures 3 and 4. The power values of the primary equipment using in the current drying system are listed in Table 2. The energy used for dehydration of corn (\dot{E}_{nevp}) and the electrical energy for lifting the corn (\dot{W}_h) are considered as the effective energy, which respectively calculated by Equations (3) and (4) [35]:

$$\dot{E}_{nevp} = \dot{m}_{evp} h_{fg} \tag{3}$$

$$\dot{W}_h = \frac{\dot{m}_{h,c} v^2}{2} + \dot{m}_{h,c} g v \tag{4}$$

Table 2. Power parameters of the primary equipment.

Equipment	Power
Hoist	5.5 kW
Discharging motor	3.75 kW
Induced fan	37 kW
Additional parts	1.5 kW

The average dehydrated moisture (m_{evp}) from corn in any period (Δt) is calculated using Equation (5):

$$\dot{m}_{evp} = \frac{m_d}{(1 - MC_t)} - \frac{m_d}{(1 - MC_{t+\Delta t})} \tag{5}$$

The latent heat of vaporization h_{fg} ($J \cdot kg^{-1}$) is calculated using Equations (6) and (7) [20]:

$$h_{fg} = 2.503 \times 10^6 - 2.386 \times 10^3 (T_g - 273.16)^{0.5} \quad 273.16 \leq T_g \leq 338.72 \tag{6}$$

$$h_{fg} = (7.33 \times 10^{12} - 1.6 \times 10^7 T_g^2)^{0.5} \quad 338.72 \leq T_g \leq 553.16 \tag{7}$$

In totally, the energy efficiency of the whole drying system can be obtained according to Equation (8)

$$\eta_{enw} = \frac{\dot{E}_{nevp} + \dot{W}_h}{\dot{Q} + \dot{P}_{if} + \dot{P}_h + \dot{P}_{dm} + \dot{P}_{ap}} \tag{8}$$

For the DC, the overall energy consuming element consist of the inlet air (\dot{E}_{nai}), the \dot{P}_{if} and the infrared recover radiator (\dot{E}_{nfir}). The effective energy is \dot{E}_{nevp} . The energy efficiency of the DC was obtained according to Equation (9):

$$\eta_{enc} = \frac{\dot{E}_{nevp}}{\dot{E}_{nai} + \dot{P}_{if} + \dot{E}_{nfir}} \tag{9}$$

From the Wien displacement law, the \dot{E}_{nfir} can be calculated using Equation (10) [36]:

$$\dot{E}_{nfir} = A_{fir} \sigma \epsilon_r T_r^4 \tag{10}$$

\dot{E}_{nai} is calculated using Equation (11) [28]:

$$\dot{E}_{nai} = \dot{m}_{ai} (h_{ai} - h_{\infty}) \tag{11}$$

The mass flow rate of the inlet dry air (\dot{m}_{ai}) can be obtained according to Equation (12) [4]:

$$\dot{m}_{ai} = \rho_{da} V S \tag{12}$$

where ρ_{da} is the density of the dry air (kg/m^3), V and S are, respectively the velocity of the inlet air (m/s) and the cross-sectional area of the inlet pipeline (m^2).

The enthalpies of the inlet and the outlet drying air (h_a) is calculated using Equation (13) [4]:

$$h_a = (C_a + \omega C_v)(T_a - T_{\infty}) + \omega h_{fg} \tag{13}$$

For the DC, the total heat loss is chiefly consisted of the heat loss in outlet air (\dot{E}_{nao}), the heat loss in outlet corn kernels (\dot{E}_{nco}) and the heat loss in chamber wall (\dot{E}_{nwall}), which can be calculated using Equation (14)–Equation (16) [28]:

$$\dot{E}_{nao} = \dot{m}_{ao}(h_{ao} - h_{\infty}) \tag{14}$$

$$\dot{E}_{nco} = C_c \dot{m}_p (T_{po} - T_{\infty}) \tag{15}$$

$$\dot{E}_{nwall} = 1.3A_s \frac{T_{wall} - T_{\infty}}{\frac{\sigma}{\gamma} + \frac{1}{1.163(6+0.5v_{\infty})}} \tag{16}$$

2.4.2. Exergy Analysis

The exergy balance equation on account of the second law of thermodynamics can be express as Equation (17) [35], which was adopted to analyze the exergy rate of each of the components of the drying system:

$$\sum \dot{E}_{xi} - \sum \dot{E}_{xo} = \sum \dot{E}_{xdes} \tag{17}$$

The chemical exergy of the coal (\dot{E}_{xfuel}) used in present works is calculated using Equation (18) [37]:

$$\dot{E}_{xfuel} = \dot{m}_{fuel} \left[0.978 + \frac{0.267O_{ar} + 0.103M_{ar}}{100 - (A_{ar} + M_{ar})} \right] \cdot LHV \tag{18}$$

In this study, the exergy of the corn and air were calculated using Equations (19)–(21) [36]:

$$E_x = (h - h_0) - T_0(s - s_0) \tag{19}$$

$$h - h_0 = c_p(T - T_0) \tag{20}$$

$$s - s_0 = c_p \ln\left(\frac{T}{T_0}\right) - R \ln\left(\frac{P}{P_0}\right) \tag{21}$$

The exergy rate of the drying medium entering and leaving the DC includes chemical exergy (ch) and physical exergy (ph), which can be expressed to Equation (22) [38]:

$$\sum \dot{x} = \sum \dot{x}^{ph} + \sum \dot{x}^{ch} \tag{22}$$

According to the previous studies [4,16,35], the physical exergy of the inlet and the outlet corn kernels (\dot{E}_{xc}) is obtained using Equation (23):

$$E\dot{x}_c^{ph} = C_c \dot{m}_c \left[(T_c - T_{\infty}) - T_{\infty} \ln\left(\frac{T_c}{T_0}\right) \right] \tag{23}$$

The physical exergy and chemical exergy rates of the drying medium was calculated using Equations (24) and (25) [35]:

$$E\dot{x}_a^{ph} = \dot{m}_a \left\{ (C_a + \omega C_v)(T_a - T_{\infty}) - T_{\infty} \left[(C_a + \omega C_v) \ln\left(\frac{T_a}{T_{\infty}}\right) - (R_a + \omega R_v) \ln\left(\frac{P_a}{P_{\infty}}\right) \right] \right\} \tag{24}$$

$$E\dot{x}_a^{ch} = \dot{m}_a \left\{ T_{\infty} \left[(R_a + \omega R_v) \ln\left(\frac{1 + 1.6078\omega_0}{1 + 1.6078\omega}\right) + 1.6078\omega R_a \ln\left(\frac{\omega}{\omega_0}\right) \right] \right\} \tag{25}$$

The exergy used for the water evaporation in the drying process (\dot{E}_{xevp}) is calculated using Equation (26) [35]:

$$\dot{E}_{xevp} = \left(1 - \frac{T_{\infty}}{T_c}\right) \dot{E}_{nevpe} \tag{26}$$

The recover radiant exergy (\dot{E}_{xfir}) recovered by the radiators can be calculated using Equation (27) [39]:

$$\dot{E}_{xfir} = A_{fir}\sigma\epsilon_r T_r^4 \left(1 - \frac{T_\infty}{T_r}\right) \tag{27}$$

Hence, the exergy efficiency of the entire drying system was calculated using Equation (28):

$$\eta_{exw} = \frac{\dot{E}_{xevp}}{\dot{E}_{xin}} = \frac{\dot{E}_{xevp} + \dot{W}_h}{\dot{E}_{xfuel} + \dot{P}_{if} + \dot{W}_h + \dot{P}_{dm} + \dot{P}_{ap}} \tag{28}$$

Additionally, the thermodynamic constants and the related technical parameters used in the present works are tabulated in Table 3.

Table 3. Some thermodynamic constants and the related technical parameters.

Parameter	Value/Equation	Unit	Reference
A_{fir}	16.6	m ²	–
σ	5.67×10^{-8}	W·m ⁻² ·K ⁻⁴	[27]
ϵ_r	0.9	–	[39]
S	0.126	m ²	–
A_s	8.3	m ²	–
δ	0.05	m	–
γ	1	W·m ⁻¹ ·K ⁻¹	–
C_c	$1.465 + 0.036 M$	kJ·kg ⁻¹ ·K ⁻¹	[40]
Ca	1.004	kJ·kg ⁻¹ ·K ⁻¹	[16]
C_v	1.872	kJ·kg ⁻¹ ·K ⁻¹	[16]
R_a	0.287	kJ·kg ⁻¹ ·K ⁻¹	[5]
R_v	0.462	kJ·mol ⁻¹ ·K ⁻¹	[5]
\dot{m}_c	9.26	kg·s ⁻¹	–

2.5. Performance Indicators

In the present work, the drying rate (DR) in any period (Δt), which reflects the strength of drying process, is calculated using Equation (29) [41]:

$$DR = \frac{M_{t+\Delta t} - MC_t}{\Delta t} \times 100\% \tag{29}$$

The energy efficiency (η_{en}) and the specific energy consumption (SEC) are utilized to assess the energetic performance of the components and the whole system. The SEC is calculated according to Equation (30) [42]:

$$SEC = \frac{\dot{Q} + \dot{P}_{if} + \dot{P}_h + \dot{P}_{dm} + \dot{P}_{ap}}{\dot{m}_{evp}} \tag{30}$$

The exergy efficiency (η_{ex}), exergy destruction ratio (r_d) [43] and stainability index (SI) [4] are utilized to assess the exergetic performance of the components and the whole system. Generally, the η_{ex} is increased with the reducing exergy destruction. SI can reflect the impact of exergy efficiency changes on sustainability while r_d can reflect the contribution level of the exergy destruction related to the component to the overall exergy destruction. All performance indicators are defined as follows:

$$r_d = \frac{\dot{E}_{xdes,k}}{\dot{E}_{xdes,tot}} \tag{31}$$

$$SI = \frac{1}{1 - \eta_{exdes}} \tag{32}$$

2.6. Uncertainty Analysis

The experimental errors and uncertainties of the current work mainly come from the dryer, instruments accuracy, environmental conditions and observation restrictions. The measurement uncertainty is adopted to describe the accuracy of the experiments, as shown below [44]:

$$U = [(\frac{\partial F}{\partial z_1} u_1)^2 + (\frac{\partial F}{\partial z_2} u_2)^2 + \dots + (\frac{\partial F}{\partial z_i} u_i)^2]^{0.5} \tag{33}$$

where U is the uncertainty in the outcome; u_1, u_2, \dots, u_i are the uncertainty in the independent variables; z_1, z_2, \dots, z_i are the independent variables and F is the function of the independent variables.

3. Results and Discussions

3.1. Drying Kinetics of the IRCC Corn Dryer

The ambient and medium conditions during drying process are depicted in Figure 5. In the current work, the drying kinetics was used to evaluate the dryer performance; the MC and DR curves are depicted in Figure 6. The ambient temperature on the test day was relatively low, with an average of 8.83 °C. The average temperature of inlet air was 107.06 °C. The humidity of inlet air was affected by the real-time environment, with a fluctuation range of 3.71–4.02 g/kg and an average value of 3.83 g/kg.

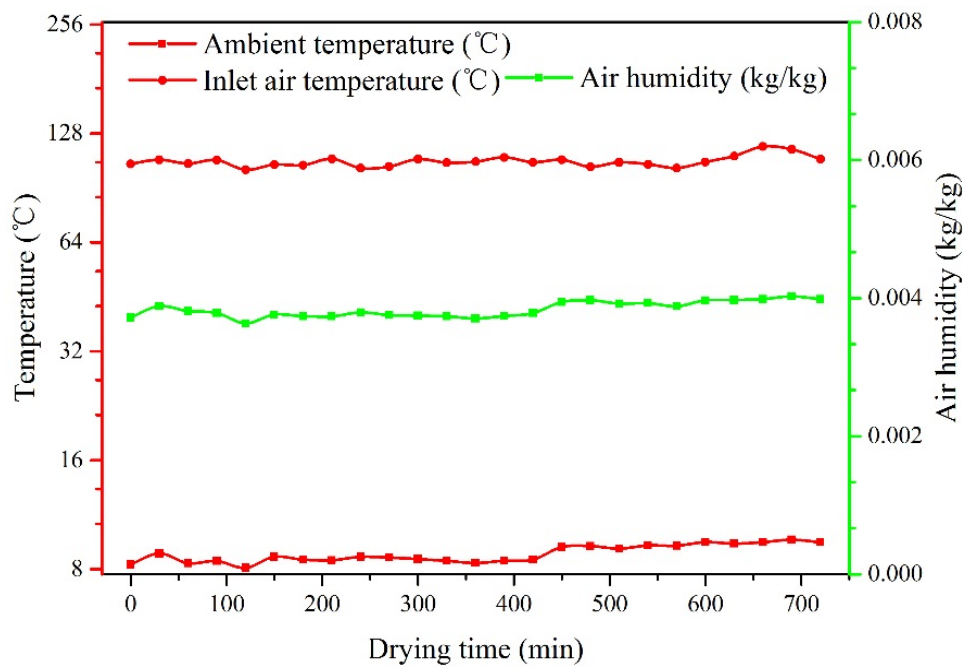


Figure 5. Ambient and medium conditions during drying process.

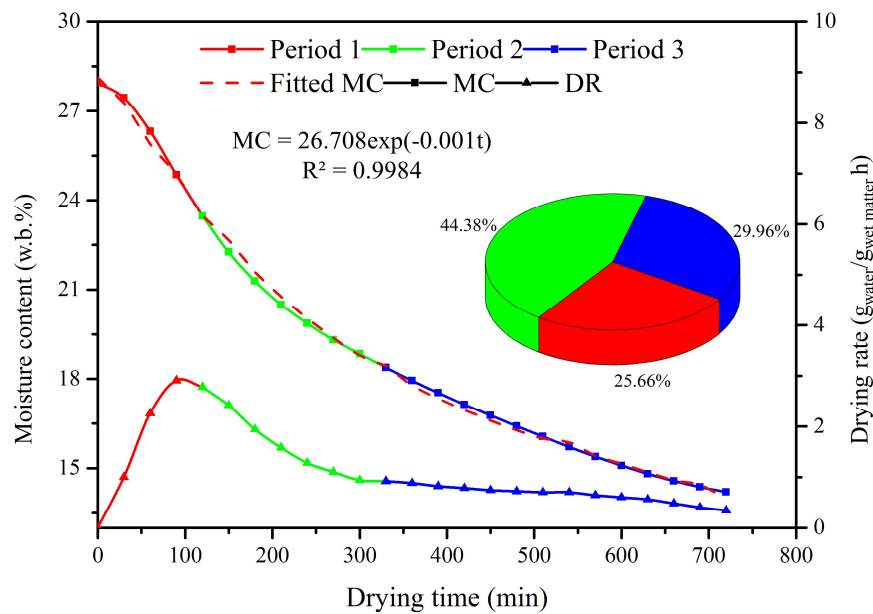


Figure 6. Kinetics curves of the corn drying process.

The results show that the corn moisture content decreased from the initial value (27.95% w.b.) to the safe value (14.2% w.b.). The whole drying process lasted for 12 h (eight circulations) with the drying capacity of 4.2 t/h. The relationship between MC and t was simulated by the experimental data, which can be described as $MC = 26.708 \exp(-0.001t)$ ($R^2 = 0.9984$). In the initial stage of drying operation, the drying rate primarily increased rapidly and then decreased gradually with the advancing of drying process. The maximum and the final drying rate were, respectively $2.91 \text{ g}_{\text{water}}/\text{g}_{\text{wet matter}} \text{ h}$ and $0.34 \text{ g}_{\text{water}}/\text{g}_{\text{wet matter}} \text{ h}$, and the average drying rate of corn drying system is $1.1 \text{ g}_{\text{water}}/\text{g}_{\text{wet matter}} \text{ h}$. Additionally, according to the drying rate, the corn drying process can be divided into three stages: warming up period, falling period I and falling period II. The amount of dehydration of drying process in four stages was 2056.162 kg, 3556.209 kg and 2044.45 kg, accounting for 25.66%, 44.38% and 29.96%, respectively, as depicted in the pie chart. The corn drying process of the developed dryer in this paper presents different characteristics in different stages as described below.

In warming up period (0–90 min), the moisture in corn with high moisture content is mainly free water, including water flowing in the capillary and adhering to the kernel [45]. Since the binding effect between free water and absolute dry matter is relatively tightly, the dehydration in this stage can be regarded as the evaporation process of free water. Hence, the partial pressure of water vapor on the corn surface increases gradually in the process that the corn temperature rises to the wet bulb temperature of drying medium [40], which results in the increasing drying rate. After the large number of free water is rapidly removed in warming up period, the moisture in corn is mainly physicochemical binding water [45], at this time, the drying process begins to go through the falling period I (90–330 min). In this period, water evaporation is limited by grain itself, and the corn drying process is the result of both surface evaporation and internal diffusion. The rate of surface evaporation depends on the size of evaporation area, and the internal water evaporation rate depends on the water diffusion of corn itself. In order to accelerate the water diffusion of grain itself, abundant energy is required to offset the binding energy between the water molecules and the attachment points while little energy is utilized to evaporate water [19], which results the reduced drying rate in this stage. With the continuous decrease of corn moisture content, the drying will experience the falling period II (after 330 min). In this period, corn is in the low-moisture region and the binding energy increases significantly with the drying process [28]. The drying rate will decrease with the decreasing partial pressure of water vapor around the grain surface. Similar results have also been found in the research to wheat [46], paddy [47] and corn [48].

3.2. Energy Analysis of Corn Drying with the IRCC Corn Dryer

3.2.1. General View of Energy Structure

Figure 7 describes the overall energy consumption proportions which demonstrate the whole dryer and the DC. The overall energy consumption of the whole dryer is primarily composed of five aspects including the coal, induced fan, discharging motor, hoist and the additional parts, which accounts for 97.57%, 1.88%, 0.19%, 0.28% and 0.08% of the total, respectively. The thermal energy given by fuel for heating drying medium accounts for most of the total energy consumption compared with the electrical energy given by power source for the other components. For the DC, the energy consumption in the inlet air, the induced fan and the recover radiant energy were studied, and the results indicated that the energy consumption in E_{ai} , E_{if} and E_{fir} , respectively, account for 91.66%, 5.86% and 2.47% of the total in the DC. Specific energy consumption is a commonly adopted index to evaluate the energy consumption in grain drying process which refers to the energy input to the drying system when 1 kg water is evaporated. It can be seen from Figure 8 that the SEC of both whole dryer and drying chamber increases continuously with drying process. Moreover, due to the binding energy as described in Section 3.1, the phenomenon that SEC of the whole dryer increases rapidly (19,844.52–42,425.59 kJ/kg) after 540 min was found obviously. Similar phenomenon has also been found in the research of a novel industrial multifield synergistic paddy dryer conducted by Li [22]. The technology of variable temperature subsection drying technology proposed by some researcher [49] may solve this problem. In the present work, the overall energy input to the whole dryer of drying process was 84,874.8 MJ, and the average SEC was 10.592 MJ/kg. The experiment of combined hot air-infrared thin layer drying of paddy studied by Zare in 2015 [50] showed that the SEC of paddy drying varied from 9.4 to 50.3 MJ/kg, which indicating that the IRCC dryer of the present work has an acceptable level of energy utilization. For the drying chamber, the total energy consumption was 27,263.962 MJ while the average SEC is 3.402 MJ/kg. Figure 9 shows that the overall energy efficiency of the entire drying system and DC respectively ranges from 2.16% to 35.21% and 4.2% to 62.11%—which is higher than some previous findings, such as the paddy-fluidized bed drying with an energy efficiency of 5.24% to 13.92% [51] or potato-slices drying with an energy efficiency of 15.13% to 37% [21].

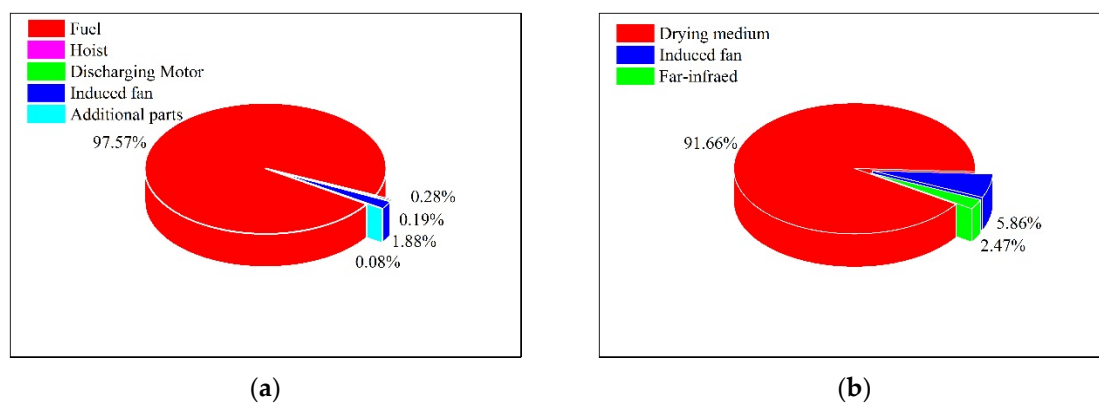


Figure 7. Assessment of overall energy consumption of (a) the entire drying system and (b) the counterflow drying chamber (DC).

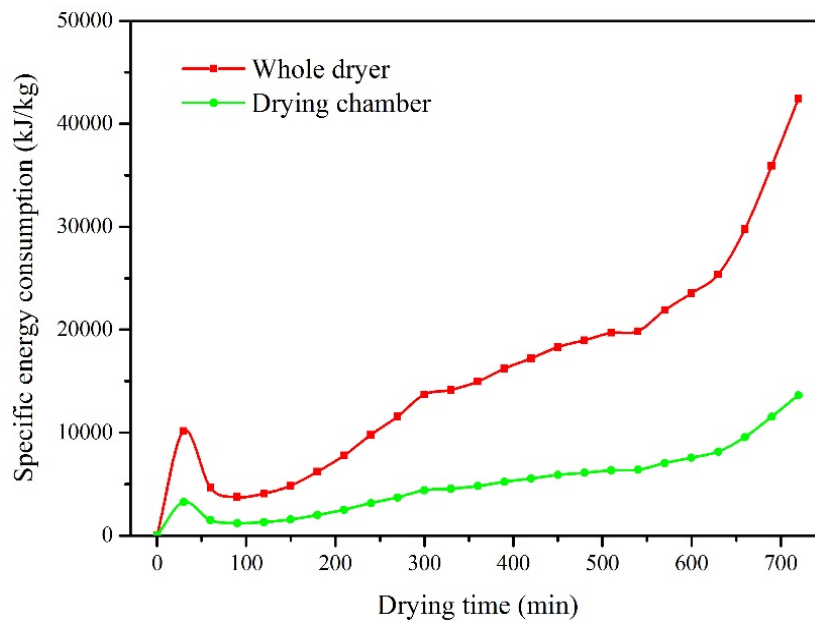


Figure 8. Variations of specific energy consumption (SEC) of the whole dryer and the DC during drying process.

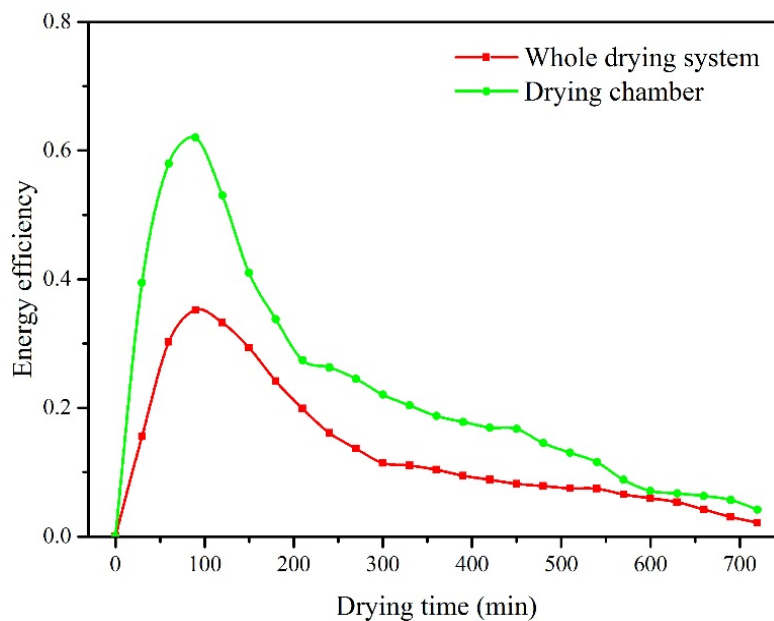


Figure 9. Variations of energy efficiency of the whole dryer and the DC during drying process.

3.2.2. Radiant Energy Recovery

In preheating section, due to the fact that the radiator was inserted in the far infrared section and surrounded by the loose corn, the total radiation angle coefficient of the device to the corn is equivalent to 1, this means, the radiation energy caused on the outer surface of the far-infrared generation device will be totally absorbed by the corn. According to the previous research results, grains tend to acquire relatively high absorptivity at near 9- μm far-infrared wavelength [52]. The far-infrared wavelength was calculated according to the Wien displacement law [36]. In the present work, the wavelength of the radiator varies from 7.68 μm to 8.3 μm , as shown in Figure 10. Moreover, during the whole drying process, the recovered radiant energy rate is between 15.578 kW and 17.2 kW, and the overall recovered radiant energy is 674,339.3 kJ, which can be utilized to dehydrate about 270.14 kg at the

present ambient temperature. The drying method proposed in this paper can not only recover the radiation energy to strengthen the drying process, but also improve the drying quality of corn.

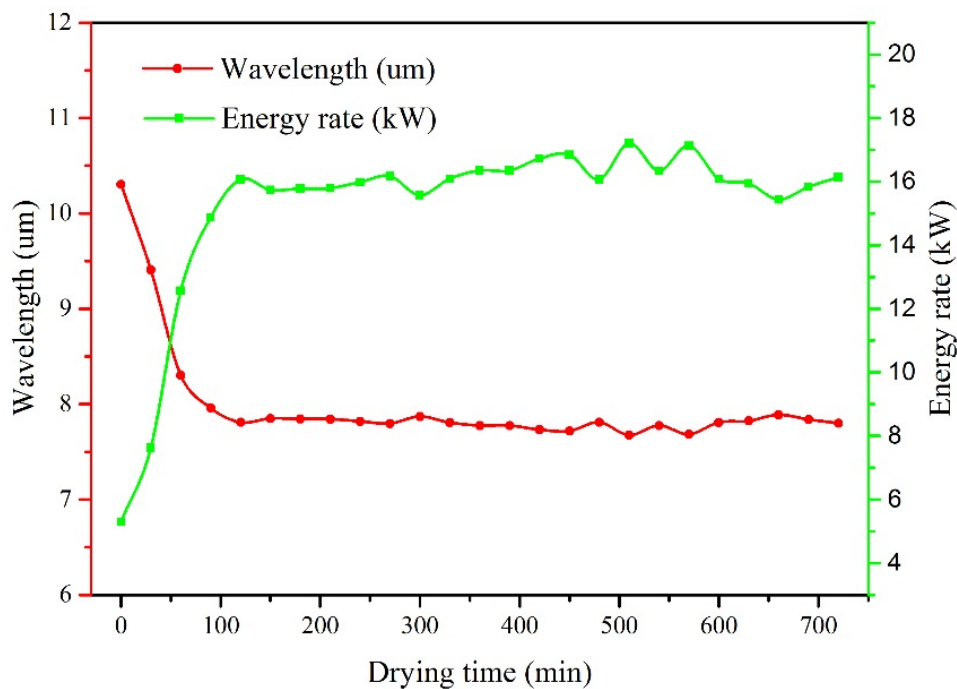


Figure 10. Variations of wavelength of the far infrared and the energy recovery process.

3.2.3. Heat Loss Characteristics

Heat loss is the primary cause of high-energy consumption and low efficiency in the grain drying process [53,54]. Hence, it is necessary to investigate the heat loss characteristics of drying process to propose scientific drying parameters and effective measures for the purpose of high-efficiency and energy savings. In the present work, heat loss characteristics—including heat loss in the outlet air, heat loss in the outlet corn and heat loss to the chamber wall—are depicted in Figure 11. The results indicated that the above three types of heat loss were calculated to be 20,045.23 MJ, 12,547.16 MJ and 5151.52 MJ, accounting for 53.11%, 33.24% and 13.65% of total, respectively, and the average heat-loss rate was learned to be 3145.26 MJ/h. The heat-loss rate in outlet air and outlet corn increased with the drying process and tended to be a constant after reaching the maximum. During the drying process, the grain flow speed and moisture content gradually decrease, which leads to small gaps among particles [55]. As a result, the effective evaporation area coefficient of the drying phase interface was reduced, and the strength of heat and mass transfer between corn and drying medium were weakened. Additionally, the heat in the drying medium is hardly fully utilized, resulting in an increasing heat-loss rate of exhaust gas. Finally, during the period of 500–600 min, the heat-loss rate in outlet air fluctuated slightly, which may result from the impact that ambient on the drying process. During the whole drying process, especially in the later stage, heat-loss rate in outlet air showed an increasing trend. Therefore, it is of great significance to design a recovery device to reuse the waste heat in the outlet air for the motivation of reducing the exhaust heat loss and energy-consumption costs. Li [56] found a similar result in his research on the characteristic analysis of heat loss in a multistage counterflow paddy dryer and pointed out that a corresponding waste heat recovery device should be designed for the problem of high-exhaust heat loss.

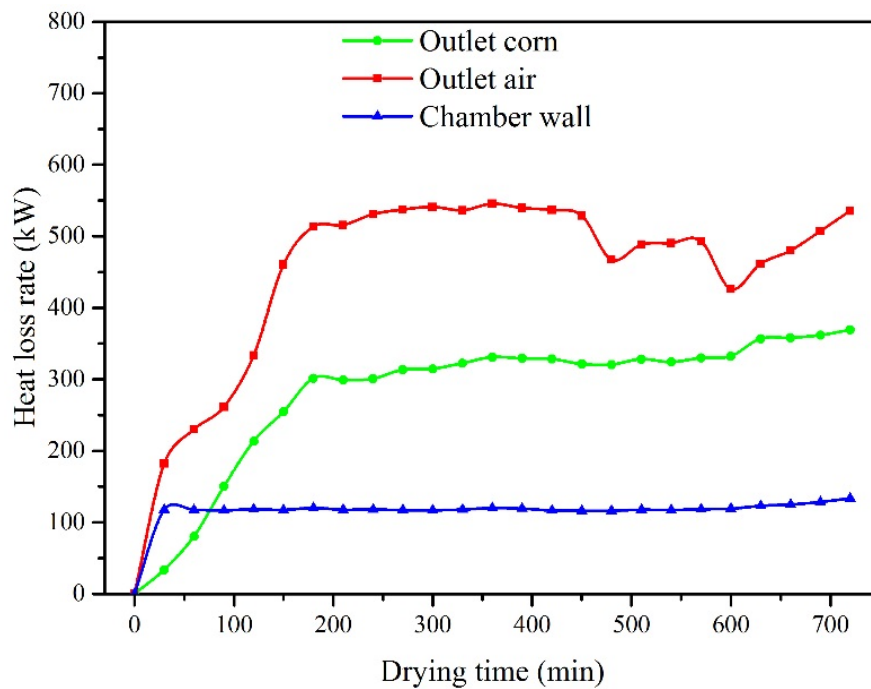


Figure 11. Variations of the heat-loss rate of the DC.

At the beginning of drying process, a great deal of heat will be taken out from the DC by the heated grains due to the relatively low ambient temperature, which caused the increase of grain temperature and heat-loss rate in outlet corn. Then, the heat-loss rate of outlet corn was stable as the grain temperature tends to a constant. The water-vapor pressure on the surface of corn with high moisture content is large, and the internal binding energy and resistance to dehydration are relatively small at the early stage. Hence, in order to reduce the heat loss of the outlet corn at this stage, a drying medium with low temperature and low humidity should be utilized. Moreover, in this way, a portion of the moisture in the grains can also be removed with a relatively low energy-consumption cost. At the end of the drying process (after 600 min), the moisture content of grain gradually decreases, which demonstrates that the binding energy of the grain is relatively small. The decrease of binding energy means that under the condition of the same energy input, increasing the internal energy of grains with low moisture content requires more energy. Therefore, the heat loss in outlet corn increased significantly. Ma's research [57] on the energy efficiency evaluation and experiments on grain counterflow drying systems based on exergy analysis found a similar result.

Heat loss to the chamber wall mainly occurred at the connection between the heat exchanger and the dryer. At the beginning of drying process, the heat-loss rate of the chamber wall increased with the increasing temperature of the chamber wall—and then tended to be constant. Due to the fact that the temperature of inlet air was relatively stable, the heat-loss rate of the chamber wall varied only slightly (116.58–133.4 kW).

3.3. Exergy Analysis of Corn Drying with the IRCC Corn Dryer

3.3.1. General View of Exergy Structure

The same amount of energy may have different effects in different systems [58]. In this section, Table 4 lists the exergetic performance of each component in the entire drying system during the corn drying process. Results showed that the SI of RA (1.11) and DC (1.86) have low values, while those of CC (2.40) and HE (5.64) are higher than 2 [4]. Lower SI means that the RA and DC are supposed to be ameliorated by adopting some measures. For CC and HE, HE shows good exergetic performance in exergy efficiency (82.28%), and due to the largest r_d , CC has substantial improvement potential. The r_d

of RA was lowest (1.23%) among the all components. In the current work, since the main component of recovering the waste energy in fuel gas is RA, moreover, r_d analysis indicated that the contribution rates to the overall exergy destruction are as below (in ascending sequence of significance): RA, HE, DC and CC. Hence, the further optimization of CC as the focus of effort is of practical significance.

Table 4. Exergetic performance of the components for the whole dryer.

Components	E_{xin} (kW)	E_{xout} (kW)	E_{xdes} (kW)	η_{ex} (%)	SI	r_d (%)	Improvement Priority
CC	2077.65	1213.38	864.27	58.40	2.40	56.11	1
HE	1213.38	1034.72	178.66	82.28	5.64	11.60	3
RA	36.34	17.39	18.95	9.74	1.11	1.23	4
DC	1001.92	523.56	478.36	46.11	1.86	31.06	2

Figure 12 presents a Sankey diagram for the exergy analyses among the four main components of the dryer. In this study, based on the relevant theory of energy–exergy methodology, the exergy brought by the reference state (② fresh air flow) was supposed as zero, which claims a starting point for the later analysis. According to this diagram, exergy rate about 2077.65 kW carried by the coal (①) was input into the CC. However, the high exergy destruction rate (864.27 kW) indicates that the CC should be vastly ameliorated by taking some measures like changing the fuel type, adding a heat-insulating layer to the CC wall and optimizing the physical architecture of the DC. For the HE, only 178.66 kW exergy is destroyed, accounting for 14.72% of the total. Moreover, the energy recovery by the far-infrared section further improves the exergy efficiency. The above discussions indicate that the HE has excellent performance in aspect of exergy. Li [59] conducted a more detailed description of the self-developed heat exchanger used in the present project. For the RA, a 3.54-kW exergy rate was recovered by the radiators (⑥), accounting for 0.17% of the overall exergy input rate. Although this amount is quite small compared to the overall input exergy, the influence of infrared radiation has a significant performance on improving the quality of the maize kernels, as discussed in Section 3.2.2. For the DC, the average exergy rate for evaporating water was ascertained to be 462 kW (⑧), which accounts for 46.27% of the overall exergy rate inputting into the drying chamber (⑦). Furthermore, a high exergy destruction rate (478.36 kW) was found clearly in the DC, indicating the exergy performance of drying chamber can be vastly optimized.

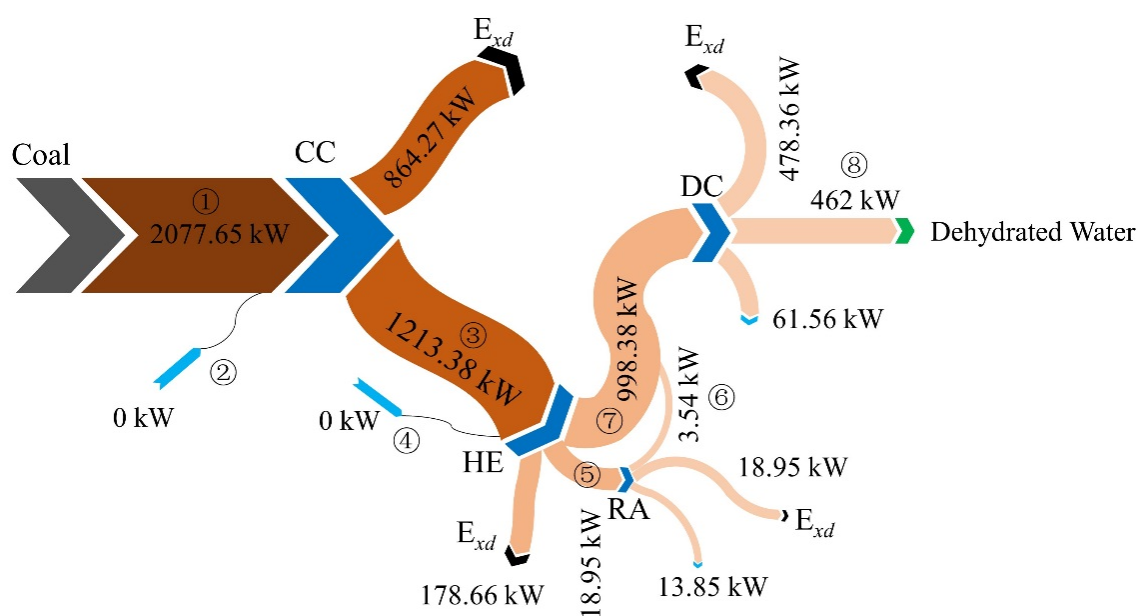


Figure 12. Sankey diagram of the overall drying system assisted by the exergy analysis.

3.3.2. Exergetic Performance

Figure 13 shows the variation of η_{ex} and SI with drying process for the purpose of comprehensively determining the energy performance of DC and the entire drying system during the complete drying process. The result indicates that η_{ex} and SI of the whole drying system decrease with the advancing of drying process and vary from 5.16% to 38.21% and 1.05 to 1.61, respectively. These results are close to those in similar agricultural product industrial dryers, such as an industrial tray dryer for cassava-starch drying ($16.04\% \leq \eta_{ex} \leq 30.65\%$; $1.19 \leq SI \leq 1.44$) [1] and a convective dryer for rough rice drying ($5.1\% \leq \eta_{ex} \leq 29.4\%$; $1.05 \leq SI \leq 1.42$) [4]. Compared with the entire drying system at a time, the values of η_{ex} and SI of DC are correspondingly higher. In terms of the heat loss characteristics investigated in Section 3.2.3, in the initial stages of the drying process, the heat loss of DC is relatively low; hence, η_{ex} reaches a maximum in this period, due to the fact that the decrease of heat loss means an increase of both energy and exergy efficiency. After 9 h, the relatively low η_{ex} (less than 20%) of DC indicates that measures should be applied to strengthen the drying kinetic. Low-temperature drying may be a feasible method to solve the problem of low-exergy efficiency in the latter stage of drying [51].

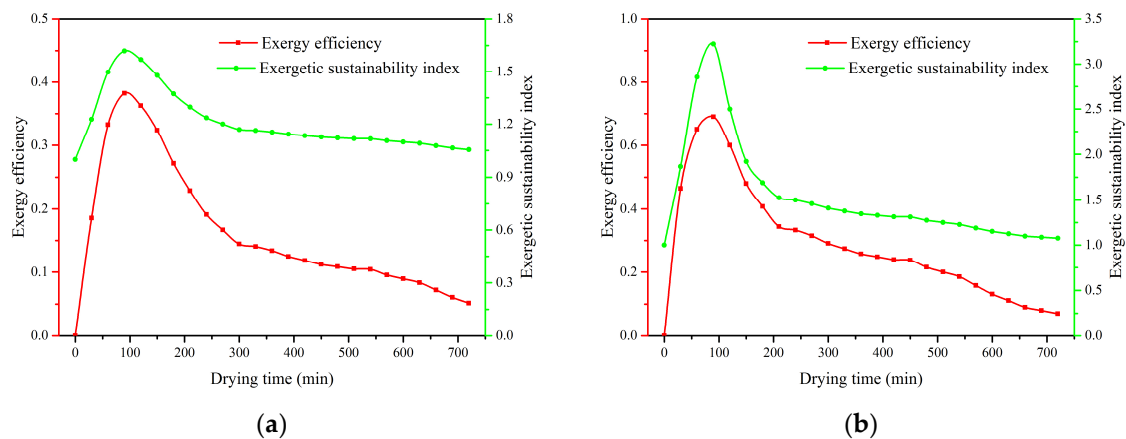


Figure 13. Variations of η_{ex} and SI with the drying process of (a) the whole drying system and (b) the DC.

4. Conclusions

This research describes a detailed study undertaken to investigate the energy and exergy performance of a combined IRCC corn dryer. The key findings according to the results of the research can be summarized as below:

- (1) The average drying rate of corn drying system in the current dryer was $1.1 \text{ g}_{\text{water}}/\text{g}_{\text{wet matter}} \cdot \text{h}$. According to the drying rate, the drying process of corn can be divided into three stages; the dehydration of each stage accounts for 25.66%, 44.38% and 29.96% of total, respectively;
- (2) The energy efficiency of the entire drying system ranged from 2.16% to 35.21%. Additionally, the SEC of the whole drying system increases rapidly (19,844.52–42,425.59 kJ/kg) due to the effect of the binding energy after 540 min, indicating that energy efficiency ought to be optimized in this period;
- (3) The overall recovered radiant energy and the average radiant exergy rate were 674,339.3 kJ and 3.54 kW, respectively. Moreover, the wavelength range of the radiator with slight fluctuation (between $7.68 \mu\text{m}$ and $8.3 \mu\text{m}$) indicated that the corn quality has been improved correspondingly under the suitable far-infrared radiation absorption rate;
- (4) Heat loss in the outlet air, the corn kernels and to the chamber wall were found to be 20,045.23 MJ, 12,547.16 MJ and 5151.52 MJ, accounting for 53.11%, 33.24% and 13.65% of the total, respectively. It is of great significance to design a waste-heat recovery device in view of reducing exhaust heat-loss and energy-consumption costs—especially in the later stages of the drying process.

- (5) The average exergy rate for dehydration was 462 kW; the exergy efficiency of the whole drying system varied from 5.16% to 38.21%, indicating that the IRCC corn dryer had a productive exergy performance;
- (6) Measures should primarily be put in place to optimize the CC, below by the DC, HE and RA according to the contribution level to the total exergy destruction.

The present work revealed the performance evaluation of the IRCC corn dryer regarding energy consumption. The main conclusions of the present work may help to better understand the energy system of the drying system and scientifically guiding the design of the drying equipment. Further research is recommended to develop the optimum controller of industrial grain drying system based on the theoretical basis provided by the present work to obtain the higher quality corn at acceptable energy consumption.

Author Contributions: Methodology, C.L. (Chengjie Li) and B.L.; software, C.L. (Chengjie Li) and J.H.; writing—original draft preparation, C.L. (Chengjie Li); supervision, project administration, C.L. (Changyou Li); data curation, C.L. (Chengjie Li), B.L. and J.H. The final version of the manuscript was reviewed and agreed by all authors. All authors have read and agreed to the published version of the manuscript.

Funding: This project was funded by the National Natural Science Foundation of China (no. 31671783; no. 31371871) and Science and Technology Planning Project of Guangdong Province, China (no. 2014B020207001).

Acknowledgments: The authors would like to thank to the editors and reviewers for their valuable and constructive comments.

Conflicts of Interest: The authors declare that we have no known competing financial interests or personal relationships that could have appeared to influence the work reported in this paper.

Nomenclature

c	specific heat ($\text{J}\cdot\text{kg}^{-1}\cdot\text{K}^{-1}$)
ω	humidity ratio of air ($\text{kg water vapor/kg dry air}$)
\dot{m}	mass flow rate ($\text{kg}\cdot\text{s}^{-1}$)
\dot{E}_n	energy rate (kW)
\dot{E}_x	exergy rate (kW)
\dot{Q}	heat transfer rate (kW)
\dot{P}	power rate (kW)
\dot{W}	work rate (kW)
R	gas constant ($\text{kJ}\cdot\text{kg}^{-1}\cdot\text{K}^{-1}$)
A_{fir}	cross-sectional area of the drying chamber (m^2)
v	velocity ($\text{m}\cdot\text{s}^{-1}$)
g	gravity acceleration ($\text{m}\cdot\text{s}^{-2}$)
h_{fg}	latent heat ($\text{kJ}\cdot\text{kg}^{-1}$)
T	temperature (K or $^{\circ}\text{C}$)
m	mass (kg)
m_d	dry weight (kg)
p_i	pressure (Pa)
h	specific enthalpy ($\text{kJ}\cdot\text{kg}^{-1}$)

Abbreviations

IRCC	infrared radiation–counterflow circulation
IR	infrared radiation
TP	tempering section
IRD	infrared radiation section
DC	drying chamber
DCS	discharging section
HE	heat exchanger
CC	combustion chamber
MC	moisture content
RA	Radiators

Greek Symbols

ε	emissivity
ρ	density (kg·m ³)
μ	dynamic viscosity (kg·m ⁻¹ ·s ⁻¹)
γ	thermal conductivity (W·m ⁻¹ ·K ⁻¹)
δ	thickness (m)
λ	wavelength (um)

Subscripts

<i>a</i>	air
<i>g</i>	corn kernels
<i>in</i>	inlet
<i>out</i>	outlet
<i>v</i>	vapor
<i>c</i>	chamber
∞	ambient
<i>r</i>	radiator
<i>wall</i>	<i>dryer wall</i>
<i>h</i>	hoist
<i>dm</i>	discharging motor
<i>if</i>	induced fan
<i>ap</i>	additional parts
<i>evap</i>	evaporation
(Δt)	time
<i>da</i>	dry air

References

1. Aviara, N.A.; Onuoha, L.N.; Falola, O.E.; Igbeka, J.C. Energy and exergy analyses of native cassava starch drying in a tray dryer. *Energy* **2014**, *73*, 809–817. [[CrossRef](#)]
2. Midilli, A.; Kucuk, H. Energy and exergy analyses of solar drying process of pistachio. *Energy* **2003**, *28*, 539–556. [[CrossRef](#)]
3. Defraeye, T. Advanced computational modelling for drying processes—A review. *Appl. Energy* **2014**, *131*, 323–344. [[CrossRef](#)]
4. Beigi, M.; Tohidi, M.; Torki-Harchegani, M. Exergetic Analysis of Deep-Bed Drying of Rough Rice in a Convective Dryer. *Energy* **2017**, *140*. [[CrossRef](#)]
5. Tohidi, M.; Sadeghi, M.; Torki-Harchegani, M. Energy and quality aspects for fixed deep bed drying of paddy. *Renew. Sustain. Energy Rev.* **2017**, *70*, 519–528. [[CrossRef](#)]
6. Ozgen, F.; Celik, N. Evaluation of Design Parameters on Drying of Kiwi Fruit. *Appl. Sci.* **2019**, *9*, 10. [[CrossRef](#)]
7. Zheng, X.; Liu, H.; Shen, L.; Wang, J.; Wang, L.; Zhu, Y. Hot-air Drying Technology of Changing Temperature for Paddy Rice Based on Glass Transition Theory. *Trans. Chin. Soc. Agric. Mach.* **2020**, *51*, 331–340. [[CrossRef](#)]
8. Romuli, S.; Schock, S.; Somda, M.K.; Müller, J. Drying Performance and Aflatoxin Content of Paddy Rice Applying an Inflatable Solar Dryer in Burkina Faso. *Appl. Sci.* **2020**, *10*, 3533. [[CrossRef](#)]
9. Taechapiroj, C.; Dhuchakallaya, I.; Soponronnarit, S.; Wetchacama, S.; Prachayawarakorn, S. Superheated steam fluidised bed paddy drying. *J. Food Eng.* **2003**, *58*, 67–73. [[CrossRef](#)]
10. Li, C.; Mai, Z.; Fang, Z.; Zhang, Y. Design and test on energy-saving drying system for paddy with high moisture content. *Trans. Chin. Soc. Agric. Eng.* **2014**, *30*, 1–9. [[CrossRef](#)]
11. Xie, Y.; Zhang, Y.; Xie, Y.; Li, X.; Liu, Y.; Gao, Z. Radio frequency treatment accelerates drying rates and improves vigor of corn seeds. *Food Chem.* **2020**, *319*, 126597. [[CrossRef](#)] [[PubMed](#)]
12. Faria, R.Q.D.; Santos, A.R.P.D.; Garipey, Y.; Silva, E.A.A.D.; Maria, M.P.S.; Raghavan, V. Optimization of the process of drying of corn seeds with the use of microwaves. *Dry. Technol.* **2020**, *38*, 676–684. [[CrossRef](#)]

13. Li, S.; Chen, S.; Liang, Q.; Ma, Z.; Han, F.; Xu, Y.; Jin, Y.; Wu, W. Low temperature plasma pretreatment enhances hot-air drying kinetics of corn kernels. *J. Food Process Eng.* **2019**, e13195. [[CrossRef](#)]
14. Vera, I.; Langlois, L. Energy indicators for sustainable development. *Energy* **2007**, *32*, 875–882. [[CrossRef](#)]
15. Li, C.; Ma, X.; Fang, Z.; Zhang, Y. Thermal energy structure of grain hot air drying and analytical method. *Trans. Chin. Soc. Agric. Eng.* **2014**, *30*, 220–228. [[CrossRef](#)]
16. Khanali, M.; Aghbashlo, M.; Rafiee, S.; Jafari, A. Exergetic performance assessment of plug flow fluidised bed drying process of rough rice. *Int. J. Energy* **2013**, *13*, 387–408. [[CrossRef](#)]
17. Dincer, I. On energetic, exergetic and environmental aspects of drying systems. *Int. J. Energy Res.* **2002**, *26*, 717–727. [[CrossRef](#)]
18. Moran, M.J.; Shapiro, H.N. *Fundamentals of Engineering Thermodynamics*, 6th ed.; John Wiley and Sons Inc.: Chichester, UK, 2000. [[CrossRef](#)]
19. Yildirim, N.; Genc, S. Energy and exergy analysis of a milk powder production system. *Energy Convers. Manag.* **2017**, *149*, 698–705. [[CrossRef](#)]
20. Aghbashlo, M.; Mobli, H.; Rafiee, S.; Madadlou, A. Energy and exergy analyses of the spray drying process of fish oil microencapsulation. *Biosyst. Eng.* **2012**, *111*, 229–241. [[CrossRef](#)]
21. Aghbashlo, M.; Kianmehr, M.H.; Arabhosseini, A. Energy and exergy analyses of thin-layer drying of potato slices in a semi-industrial continuous band dryer. *Dry. Technol.* **2008**, *26*, 1501–1508. [[CrossRef](#)]
22. Li, B.; Li, C.; Li, T.; Zeng, Z.; Ou, W.; Li, C. Exergetic, Energetic, and Quality Performance Evaluation of Paddy Drying in a Novel Industrial Multi-Field Synergistic Dryer. *Energies* **2019**, *12*, 4588. [[CrossRef](#)]
23. Yogendrasasidhar, D.; Setty, Y.P. Drying kinetics, exergy and energy analyses of kodo millet grains and fenugreek seeds using wall heated fluidized bed dryer. *Energy* **2018**, *151*, 799–811. [[CrossRef](#)]
24. Delgado-Plaza, E.; Peralta-Jaramillo, J.; Quilambaqui, M.; Gonzalez, O.; Reinoso-Tigre, J.; Arevalo, A.; Arancibia, M.; Paucar, M.; Velázquez-Martí, B. Thermal Evaluation of a Hybrid Dryer with Solar and Geothermal Energy for Agroindustry Application. *Appl. Sci.* **2019**, *9*, 4079. [[CrossRef](#)]
25. Darvishi, H.; Zarein, M.; Farhudi, Z. Energetic and exergetic performance analysis and modeling of drying kinetics of kiwi slices. *J. Food Sci. Technol.* **2016**, *53*, 2317–2333. [[CrossRef](#)] [[PubMed](#)]
26. Li, C.; Li, B.; Huang, J.; Li, C. Developing an online measurement device based on resistance sensor for measurement of single grain moisture content in drying process. *Sensors* **2020**, *20*, 4102. [[CrossRef](#)] [[PubMed](#)]
27. Zhou, Z. *Agricultural Materials Science*; Agriculture Press: Beijing, China, 1994. (In Chinese)
28. Li, C.; Mai, Z.; Fang, Z. Analytical study of grain moisture binding energy and hot air drying dynamics. *Trans. Chin. Soc. Agric. Eng.* **2014**, *30*, 236–242. [[CrossRef](#)]
29. Khir, R.; Pan, Z.; Salim, A.; Hartsough, B.R.; Mohamed, S. Moisture diffusivity of rough rice under infrared radiation drying. *LWT Food Sci. Technol.* **2011**, *44*, 1126–1132. [[CrossRef](#)]
30. Sharma, G.P.; Verma, R.C.; Pathare, P.B. Thin-layer infrared radiation drying of onion slices. *J. Food Eng.* **2005**, *67*, 361–366. [[CrossRef](#)]
31. Li, C.Y. Hot Blast Stove Burning Chaff and its Operation Method. Patent No. CN105757650B, 27 October 2017.
32. Li, C.Y.; Fang, Z.D.; Zheng, F. A lossless grain discharging and cleaning device. Patent NO CN105707224A, 29 June 2016.
33. *National Standards of People's Republic of China*; GB 1353-2018; Maize; State Administration for Market Regulation: Beijing, China, 2017.
34. Li, B.; Li, C.; Huang, J.; Li, C. Exergoeconomic analysis of corn drying in a novel industrial drying system. *Entropy* **2020**, *22*, 689. [[CrossRef](#)]
35. Akpınar, E.K.; Midilli, A.; Bicer, Y. The first and second law analyses of thermodynamic of pumpkin drying process. *J. Food Eng.* **2006**, *72*, 320–331. [[CrossRef](#)]
36. Li, C.Y. *Engineering Thermodynamics and Heat Transfer*; China Agricultural University Press: Beijing, China, 2012. (In Chinese)
37. Stepanov, V.S. Chemical energies and exergies of fuels. *Energy* **1995**, *20*, 235–242. [[CrossRef](#)]
38. Soufiyan, M.M.; Dadak, A.; Hosseini, S.S.; Nasiri, F.; Dowlati, M.; Tahmasebi, M. Comprehensive exergy analysis of a commercial tomato paste plant with a double-effect evaporator. *Energy* **2016**, *111*, 910–922. [[CrossRef](#)]
39. Lima, J.A.S.; Santos, J. Generalized Stefan-Boltzmann law. *Int. J. Ther. Phys.* **1995**, *34*, 127–134. [[CrossRef](#)]
40. Li, C.Y. *Analysis of Grain Drying*; Science Press: Beijing, China, 2018. (In Chinese)

41. Syahrul, S.; Hamdullahpur, F.; Dincer, I. Thermal analysis in fluidized bed drying of moist particles. *Appl. Therm. Eng.* **2002**, *22*. [[CrossRef](#)]
42. Toriki-Harchegani, M.; Ghanbarian, D.; Ghasemi-Pirbalouti, A.; Sadeghi, M. Dehydration behaviour, mathematical modelling, energy efficiency and essential oil yield of peppermint leaves undergoing microwave and hot air treatments. *Renew. Sust. Energy Rev.* **2016**, *58*, 407–418. [[CrossRef](#)]
43. Aghbashlo, M.; Rosen, M.A. Exergoeconomic analysis as a new concept for developing thermodynamically, economically, and environmentally sound energy conversion systems. *J. Clean. Prod.* **2018**, *187*, 190–204. [[CrossRef](#)]
44. Aghbashlo, M.; Tabatabaei, M.; Jazini, H. Exergoeconomic and exergoenvironmental co-optimization of continuous fuel additives (acetins) synthesis from glycerol esterification with acetic acid using Amberlyst 36 catalyst. *Energy Convers. Manag.* **2018**, *65*, 183–194. [[CrossRef](#)]
45. Zhu, W.X. *Principle and Technology of Food Drying*; Science Press: Beijing, China, 2009. (In Chinese)
46. Ding, Z.; Zhu, D.; Tao, C.; Sun, L. Study on Hot Air Drying Characteristic of High-Moisture Wheat and its Mathematical Model. *Agric. Mech. Res.* **2012**, *9*, 55–60. [[CrossRef](#)]
47. Wang, X.; Hu, Q.; Xiao, B.; Yang, D.; Liu, X. Modeling Simulation of Combined Convective and Infrared radiation in rice Drying Process. *Trans. Chin. Soc. Agric. Mach.* **2013**, *44*, 145–151. [[CrossRef](#)]
48. Wang, D.; Li, H.; Yu, F.; Wang, Z. Studies on factors effecting thin-layer drying rate of corn. *Trans. Chin. Soc. Agric. Eng.* **1993**, *9*, 102–108.
49. Xiong, S.; Sun, W.; Zhao, L. Optimization of three-stage drying of paddy. *Food Sci.* **2017**, *38*, 274–281. [[CrossRef](#)]
50. Zare, D.; Naderi, H.; Ranjbaran, M. Energy and quality attributes of combined hot-air/infrared drying of paddy. *Dry. Technol.* **2015**, *33*, 570–582. [[CrossRef](#)]
51. Sarker, M.S.H.; Ibrahim, M.N.; Aziz, N.A.; Punan, M.S. Energy and exergy analysis of industrial fluidized bed drying of paddy. *Energy* **2015**, *84*, 131–138. [[CrossRef](#)]
52. Zhu, W.; Zhang, Z. Research on characteristics of infrared absorption of grain. *Grain Storage* **2003**, *32*, 38–41.
53. Syahrul, S.; Hamdullahpur, F.; Dincer, I. Exergy analysis of fluidized bed drying of moist particles. *Exergy Int. J.* **2002**, *2*, 87–98. [[CrossRef](#)]
54. Mujumdar, A.S. An Overview of innovation in industrial drying: Current status and R&D needs. *Trans. Porous Media.* **2007**, *6*, 3–18. [[CrossRef](#)]
55. Li, T.; Li, C.; Li, C.; Xu, F.; Fang, Z. Porosity of flowing rice layer: Experiments and numerical simulation. *J. Biosyst. Eng.* **2019**, *179*, 1–12. [[CrossRef](#)]
56. Li, T.; Li, C.; Li, B.; Li, C.; Fang, Z.; Zeng, Z.; Ou, W.; Huang, J. Characteristic analysis of heat loss in multistage counter-flow paddy drying process. *Energy Rep.* **2020**, *6*, 2153–2166. [[CrossRef](#)]
57. Ma, X.; Fang, Z.; Li, C. Energy efficiency evaluation and experiment on grain counter-flow drying system based on exergy analysis. *Trans. Chin. Soc. Agric. Eng.* **2017**, *33*, 285–291. [[CrossRef](#)]
58. Zhu, M. *Exergy Analysis of Energy System*; Tsinghua University Press: Beijing, China, 1988. (In Chinese)
59. Li, C.; Mai, Z.; Fang, Z.; Li, J.; Zhang, Y. Development of Seed Circulation Drying System. *Trans. Chin. Soc. Agric. Eng.* **2014**, *45*, 242–248. [[CrossRef](#)]

